FORECASTING CONVECTIVE INITIATION BY MONITORING THE EVOLUTION OF MOVING CUMULUS IN DAYTIME GOES IMAGERY

Kristopher M. Bedka [1] *, John R. Mecikalski [2], and Todd A. Berendes [2]

[1] Cooperative Institute for Meteorological Satellite Studies, University of Wisconsin–Madison
[2] Atmospheric Sciences Department, University of Alabama in Huntsville

1. INTRODUCTION

As the resolution (in both space and time) of atmospheric observing systems increase, so does our ability to monitor and forecast aspects of mesoscale weather phenomena. One aspect that has gained increased interest is the short-term prediction of rainfall events, especially those that evolve on meso- time scales (minutes to ~3 hours), which certainly include thunderstorm convection. Because thunderstorms are accompanied by rapidly changing weather on spatial and temporal scales important to travelers, energy providers and aviation interests, and produce weather hazards and phenomena that often adversely impact professionals ranging from farmers to pilots, there is a critical need to accurately predict thunderstorm development, evolution, and movement. Hazards related to thunderstorms (lightning, hail, strong winds and wind shear) cost the aviation industry many millions of dollars annually in lost time, fuel and efficiency through delayed, cancelled and rerouted flights, as well as accidents (Mecikalski et al. 2002; Murray 2002). Therefore, increased skill in forecasting thunderstorm initiation and evolution would be beneficial to a wide variety of interests.

The premises guiding this work are: 1) the CI process is well observed by satellite as small cumulus clouds grow to the cumulonimbus scale, and 2) that processing geostationary satellite data in near real-time is an optimal means of evaluating the rapidly evolving CI process. The purpose of this study then is to evaluate, in near real-time satellite imagery, the visible (VIS) and infrared (IR) signals of CI toward the development of a CI nowcasting (0-1 hour forecasting) algorithm. In particular, processing daytime geostationary satellite imagery from the GOES-12 instrument is done to identify cumulus clouds for which CI is likely to occur in the near future.

* Corresponding Author: Kristopher M. Bedka, Cooperative Institute for Meteorological Satellite Studies, 1225 West Dayton Street, UW-Madison, Madison, WI 53706. Email: krisb@ssec.wisc.edu

The outcome is an evaluation of how sequences of VIS and IR data from GOES-12 can be used to predict CI up to 45 mins prior to its occurrence during daylight hours. The data used are 1 km VIS and 4-8 km IR imagery at 15-min frequencies. As VIS and IR data are processed, approximately 16 (14 IR) pieces of information become available for use in describing the character, growth, and evolution of convective clouds, assuming cumulus clouds can be accurately tracked within 15 min images. These pieces of information are: VIS brightness counts, IR brightness temperatures (T_B's), IR multi-spectral channel differences, and IR T_B/multi-spectral temporal trend assessments using satellite-derived winds for cloud tracking. All satellite-based parameters eventually found to be important for evaluating CI are related to important dynamic and thermodynamic aspects of convective clouds undergoing the transition into organized rain-producing systems.

The definition for CI employed in this study is the first occurrence of rainfall with greater than 30 dBZ reflectivity from a cumuliform cloud, as measured by operational, ground-based radar. This definition is appropriate given our research goal of identifying cumulus clouds likely to evolve into precipitating thunderstorms within the 0-1 hour timeframe. Satellite processing is done toward forecasting the onset of ≥ 30 dBZ rainfall echoes as indicators of thunderstorm formation by tracking (monitoring) cumulus as viewed by satellite. The 30 dBZ criterion was chosen because this level of rainfall intensity, as first attained by a cumuliform cloud, has been well correlated with the eventual development of more mature cumulonimbus clouds (see Roberts and Rutledge 2003, RR03 hereafter).

The following sections will describe the analysis techniques utilized to produce a satellite-based CI nowcast. Results from the 4 May 2003 convective event over the U.S. Southern Plains will be shown to demonstrate the CI nowcast product.

2. DATASETS AND METHODOLOOGY

The satellite datasets used within this study are 1 km resolution VIS imagery and 4-8 km IR imagery from the GOES-12 Imager at a 15-min temporal resolution. For this study, the GOES-12 Imager IR data are interpolated to the 1 km VIS resolution. In doing this, the IR analysis techniques can be directly combined with the 1 km VIS data in ways that preserve the high detail and value the VIS data provide to the CI nowcast problem.

The UW-CIMSS satellite-derived wind (or atmospheric motion vector (AMV)) algorithm is used to track cloud features over a three-image sequence of GOES imagery. Through cumulus cloud tracking, IR cloud-top trends can be assessed. The methodology used in this process is described below in section 2.3.

CI nowcasts quality is determined through comparison against "truth" provided by regional mosaics of Weather Surveillance Radar-1988 Doppler (WSR-88D) data. Visual comparisons between composite reflectivity data and the CI nowcast product are performed to qualitatively identify the locations of "correct" satellite-based CI nowcast pixels (i.e. pixels where reflectivity increased to greater than 30 dBZ 30-45 mins after the nowcast was produced).

Each CI-relevant field developed from VIS and IR data can be referred to as an "interest field", with the knowledge that each field will contribute some useful information toward forecasting CI. Certainly, not all CI interest fields provide the same level of information (value) to a CI nowcast, as will be explained below. The following discussion will explain each interest field and its contribution to the CI nowcast algorithm. The reader is also referred to Mecikalski and Bedka (2004) and Bedka and Mecikalski (2004) for a more detailed description.

2.1 Convective Cloud Classification

The formation of a satellite-based convective cloud mask is the first step in the development of a CI nowcast. IR-based CI interest fields are computed only where convective clouds are present, thereby excluding approximately 70-90% (on average) of a given satellite image from further processing. This step greatly reduces the time required to produce a CI nowcast, which allows for nowcasting in near real-time.

The convective cloud mask is based upon a multi-spectral region growing (clustering) technique for classifying all scene types in a GOES image. GOES pixels are clustered based upon statistical similarity. The similarity threshold for each GOES channel is user specified and is adjusted automatically based upon standard deviation. The thresholds chosen for each satellite channel determine how many clusters (i.e. scene types) are created. Currently, we have chosen thresholds that produce 11 clusters. These clusters include "uncertain" (i.e. pixels that do not fall into any cluster), land, water, snow, stratus/fog, semi-transparent cirrus, and 5 categories of convectively induced clouds.

A database of labeled clusters is created from a set of VIS and IR training images over the area(s) of interest. The labeled cluster database forms the basis of the pixel classification technique. Pixels are assigned to a cluster based on the relationship between the pixel's multi-spectral properties and those of the clusters identified in the database.

This classification system is produced at the 1 km GOES VIS resolution and currently identifies 5 types of convectively-induced clouds: 1) small, low-level cumulus, 2) mid-level cumulus, 3) mature cumulus clouds with depths extending through the entire troposphere, 4) thick anvil ice clouds, and 5) thin anvil and cirrus clouds. For CI nowcasting purposes, analysis is primarily focused on low- to mid-level cumulus pixels, as these clouds likely have not begun to precipitate.

2.2 Band-Differencing Techniques

IR multi-spectral band differencing techniques are used here to further identify cumulus in a pre-CI state. An analysis comparing IR band differences to WSR-88D radar base reflectivity was performed for several case events (not presented in this study; the dependent data set) to identify the band difference values present before immature cumulus clouds evolved into rain-producing convective storms. From this analysis, IR band difference relationships for cumulus in a pre-CI state were formed. These values are subsequently used as CI interest fields within the nowcast algorithm, and are tested on the case described in the Section 3.

The 6.5-10.7 μm differencing technique is useful for determining the cloud-top height relative to the tropopause, or to very dry mid- and upper-tropospheric air. Positive values of the water vapor-IR window temperature difference have been shown to correspond with convective cloud tops that are at or above the tropopause (i.e. overshooting tops) in AVHRR and HIRS-2 (Ackerman 1996) and in METEOSAT-7 (Schmetz

et al. 1997) data. For the assessment of pre-CI signatures, convective clouds with positive differences have likely already begun to precipitate, especially in tropical atmospheres that support warm-top convection. Therefore, clouds with moderately negative difference values (-35 to -10 C) represent a useful CI interest field and imply the presence of low to mid-level cloud tops (~85-50 kPa).

2.3 Evaluation of Cloud-Top Trends

RR03 found that monitoring the drop in satellite-detected 10.7 μm T_B from 0° to -20° C, in addition to cooling rates of -8° C over 15 mins (their "vigorous growth" criteria), are important precursors to storm initiation for the cases examined in their study. A cooling rate of -4° C per 15 mins corresponds to "weak growth" of cumulus clouds. It was inferred by RR03 that once clouds grow to a height where cloud tops radiate at subfreezing T_B's, the ice nucleation process initiates and the development of precipitation occurs in cold-type continental clouds.

An important relationship was observed between satellite and radar data during this critical period. Following the drop to 0° C on satellite, approximately 15 mins elapsed before a precipitation echo (> 5 dBZ) was detected on radar. As clouds continued to cool, an additional 15 mins elapsed before echoes greater than 30 dBZ were observed. Reflectivities greater than 35 dBZ are typical thresholds used to track the movement of thunderstorms by the NCAR Auto-Nowcaster (Mueller et al. 2003). Therefore RR03 conclude that, by monitoring via satellite both cloud-top cooling rates and the occurrence of subfreezing 10.7 μm T_B's, the potential for up to 30 min advance notice of CI, over the use of radar alone, is possible.

The algorithm presented in this study extends the work of RR03 by incorporating the ability to evaluate trends associated with moving cloud features. To calculate cloud-top T_B trends, RR03 performed a "per-pixel" differencing technique in which the cloud-top T_B from a given satellite pixel is subtracted from the T_B at the same pixel in previous imagery. However, if a cloud feature is moving, the per-pixel technique will misrepresent true cloud trends by producing spurious T_B fall (rise) couplets in the new (previous) cloud location.

In order to account for cloud motion in the time interval between satellite images, this study incorporates the UW-CIMSS satellite-derived cloud-motion VIS and IR AMV algorithm (Velden

et al. 1997, 1998) toward the formation of satellite-derived offset vectors (SOVs) for evaluating cloud-top TB and multi-spectral band difference trends. A SOV is a measure of the distance that a cumulus cloud pixel has traveled (in pixels) between successive satellite images.

Initialization settings associated with AMV algorithm were manipulated in a way that allows for the identification of both synoptic- and meso-scale flows. The AMV algorithm used in operational settings preferentially identifies synoptic-scale flow in geostrophic balance. Adjustments were made to 1) reduce the impact of the NWP model background, 2) increase the number of cloud features tracked, 3) change the AMV editing methodology for optimal meso-scale AMV detection. These changes all serve to enhance detection of meso-scale cloud motions associated with boundary layer (upper-tropospheric) convergence (divergence) that can be used to more accurately obtain cloud-top trend information.

Once the AMVs are obtained, a Barnes objective analysis (Barnes 1964) is performed to produce a satellite wind analysis at 1-km resolution for three atmospheric layers, 100-70 kPa, 70-40 kPa, and 40-10 kPa. Convectively-induced cloud pixels are assigned an AMV from one of the three layers depending on a comparison of the pixel 10.7 μm T_B and a NWP model temperature profile. Cloud-top trends are calculated if a satellite wind is present at the appropriate height within the near vicinity of a cumulus cloud (~0.25° radius). The wind speed, direction, and the time interval between images are used to obtain the SOV and thus the approximate pixel/cloud location in previous images.

After applying the SOV, a check is performed to ensure that the past pixel location does in fact represent a convectively-induced cloud. Assuming a pixel passes both checks (wind availability and past cloud presence) for both the 15- and 30-min time lags, cloud-top cooling/multi-spectral band difference trends are calculated. The passage of these checks therefore indicates that a convectively induced cloud is being tracked, back to a reasonable prior location, across successive images.

Four interest fields result from the analysis of 10.7 μm cloud-top cooling rates, in correspondence with the results of RR03: 1) cloud-top cooling rates greater than 4° C/15 mins that 2) have exhibited sustained cooling for a 30 min period (ΔT_B/30 mins > ΔT_B/15 mins) and 3) below freezing cloud-top T_B's that 4) have dropped

from above to below freezing within the t to t-30 min time interval. The weaker of the two RR03 cooling rates (4° C vs. 8° C) was selected in order to provide a conservative identification of clouds that may be slowly evolving into cumulonimbus.

In addition to being able to use 15 and 30 min cloud-top cooling rates for CI assessment, we have also utilized SOVs to perform trend assessments of the 6.5-10.7 µm multi-spectral technique [i.e. Δ(6.5-10.7 µm)/dt] for moving convection. As the 6.5-10.7 µm channel difference is typically negative, except in the presence of deep, cold clouds, the time trend of this quantity will be positive for growing cumulus. Positive time trends in 6.5-10.7 µm channel differences imply that a cloud top is growing into increasingly dry air in middle or especially upper tropospheric levels, and is getting closer to the local equilibrium level/tropopause. Larger values of Δ(6.5-10.7 µm)/dt indicate more rapid cloud deepening. Should this time trend become negative, it indicates diminished deepening or a decreasing cloud-top height.

Temporal trend values of this multi-spectral difference $\geq 3°$ C/15 mins were observed to precede CI in the dependent data set. Unlike most of the other CI interest fields, the lack of past research using this indicator provides no comparable study to support or refute the "critical" values chosen as a CI interest field. Nonetheless, it is felt that this IR indicator offers a degree of non-redundant information, and is therefore incorporated into the CI nowcast algorithm.

2.4. CI Nowcast Technique

In order to provide CI nowcasts using VIS and IR satellite indicators, a scoring system is developed that incorporates the interest fields described above as a simple sum of positive indicators for the occurrence of CI. It is important to restate that each IR-based CI interest field used in the scoring is related to the physics of cloud growth and glaciation related to precipitation formation in cumuliform clouds, and thus describes the time-evolution of the CI process from an IR perspective. Satellite pixels that meet at least five of six CI criteria have been determined to represent rapidly growing, immature (non-precipitating) cumulus in a pre-CI state. The underlying assumption in this nowcasting system is that immature cumulus exhibiting recent signs of rapid development will continue to evolve into precipitating convective storms, provided that the cloud has access to sufficient ABL/elevated moisture.

3.   RESULTS

A strong, slow-moving spring storm served as the focal point for a severe thunderstorm outbreak across much of the U.S. Southern Plains on 4 May 2003. At least 94 tornadoes touched town in eight states including 39 in Missouri, 17 in Tennessee, 15 in Kansas, and 9 in Arkansas within this event (according to SPC storm reports), along with many reports of hail and high winds. Attention will focus on the time period from 1930-2100 UTC as convective storms were rapidly developing throughout the state of Kansas.

A comparison of the convective cloud classification to GOES-12 VIS imagery at 2000 UTC is provided in Figure 1.   This algorithm performs quite well in identifying various types of convectively-induced clouds. A comparison of the classification image to WSR-88D composite reflectivity imagery, shown in Figure 2, illustrates that that the mature cumulus and thick anvil ice clouds correspond with precipitation echoes, whereas the low- to mid-level cumulus do not.
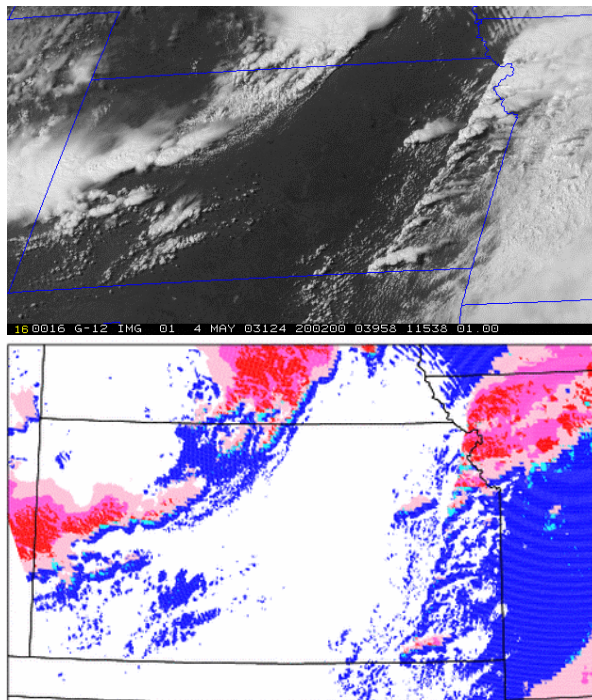

Figure 1: (top) 1 km resolution GOES-12 visible imagery at 2000 UTC on 4 May 2003. (bottom) The convective cloud classification, where blue is small low-level cumulus and thin water cloud, cyan is mid-level cumulus, red is mature cumulus, magenta is thick anvil ice cloud, and pink is thin anvil ice cloud.
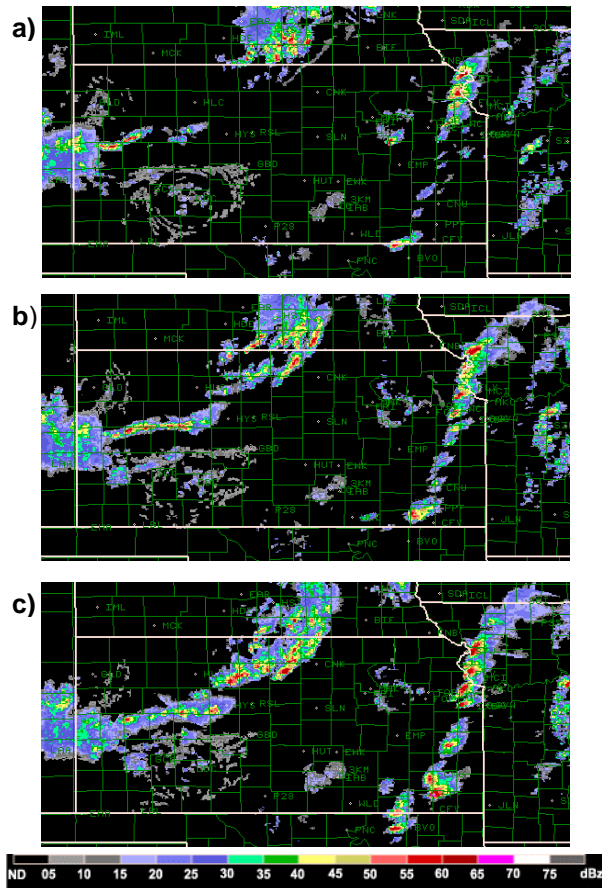
Figure 2: WSR-88D composite reflectivity mosaics at: (a) 2000 UTC, (b) 2030 UTC, and (c) 2100 UTC on 4 May 2003 illustrating the evolution of the thunderstorms across Kansas [courtesy of National Center for Atmospheric Research, Research Applications Program (NCAR-RAP)].
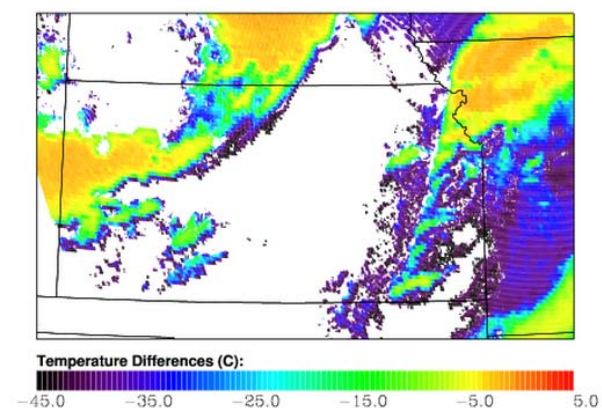

Figure 3: The 6.5-10.7 μm spectral band differencing technique at 2000 UTC on 4 May 2003.

An example of the 6.5–10.7 μm difference technique is shown in Figure 3. Difference values greater than –10º C are found to correspond well with mature cumulus and both categories of anvil ice clouds. As previously stated, clouds with tops near the tropopause need not be monitored for future CI. Clouds with moderately negative values, –35 to –10º C, correspond well with low- to mid-level cumulus that have either not begun to precipitate or have reflectivities below the 30 dBZ CI threshold.

Figure 4 shows the AMVs derived using three 15-min resolution images from 1930-2000 UTC. The aforementioned adjustments to the AMV identification software resulted in an approximately 2000% increase (3516 vs 152 vectors) in the number of AMVs found within this image sequence over operational AMV identification techniques. AMVs within the 100-70 kPa layer (1178 vectors) are used for tracking of immature, non-precipitating cumulus, whereas AMVs within the 70-40 kPa (1283 vectors) and 40-10 kPa (1055 vectors) layers are used for tracking of newly developing and mature cumulus/cirrus, respectively.

A comparison between the mesoscale AMV field and regional radiosonde observations (not shown) indicates that the vast majority of the mesoscale AMV possess reasonable speed and direction within all three atmospheric layers, given the caveats that the radiosonde observations were collected four hours later than the AMVs and that weather balloons are moving measurement platforms that propagate with the atmospheric flow (eastward in this case) during ascent.

30-min 10.7 μm cooling estimates with and without the use of meso-scale AMVs are shown in Figure 5c-d. A comparison of Fig. 5c and 5a reveals that accurate cooling estimates can be achieved using the aforementioned cloud-top trend assessment technique. Comparison between Fig 5c and 5d yields differences in both location and magnitude of cooling maxima, especially in the south-west and north-east portions of this domain. Fig. 5d indicates that many convective clouds in southwest Kansas exhibit cooling rates greater than 40º C. An examination of Fig. 5a reveals that these rates are much greater than those that actually occurred, with the disparity caused by the movement of convective cloud features within the 30-min period between these two images. The results without using meso-scale AMVs will only represent the true cooling rates important for CI nowcasting (located near the primary updraft) when convective storms are stationary, which is not the case for most clouds in this domain.

Satellite Winds (40-10 kPa)

a)

Satellite Winds (70-40 kPa)

b)

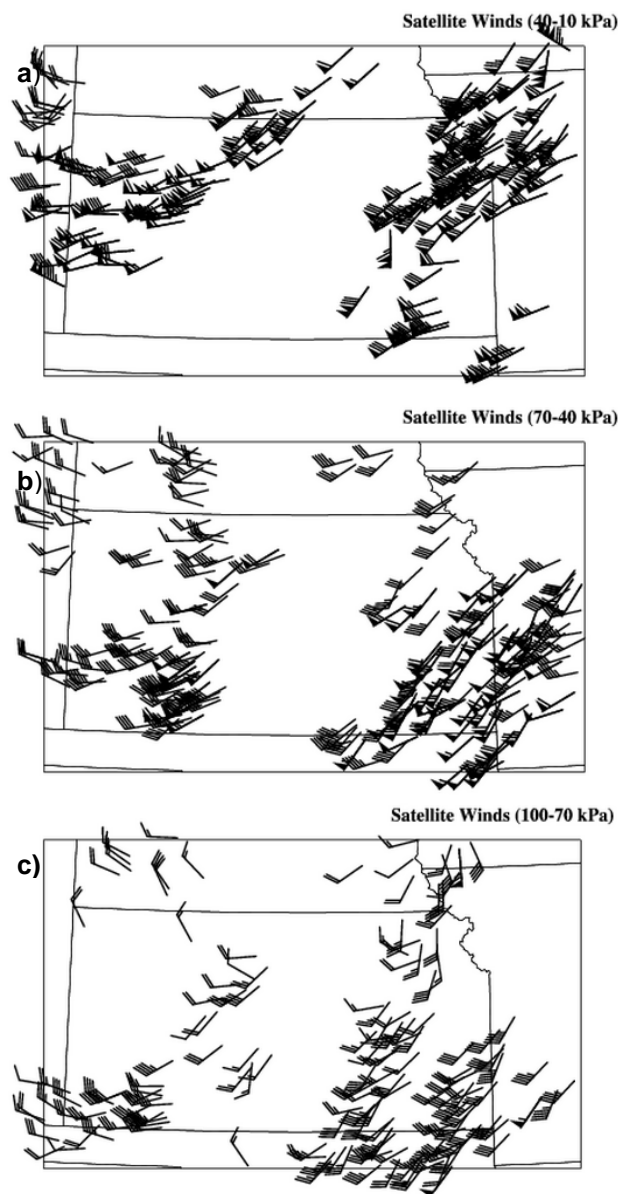**Satellite Winds (100-70 kPa)**

c)

Figure 4: (a) The satellite-derived AMV field (in knots) within the 40-10 kPa layer. Only 20% of the winds are shown for clarity. (b) Same as (a) but for the 70-40 kPa layer. (c) Same as (a) and (b), but for the 100-70 kPa layer.

A nowcast of future CI can be produced by combining the six CI interest fields summarized in Figure 6. Pixels that meet at least five of the six CI interest field criteria have been highlighted in red in Figure 6, and provide a forecast of CI over the following 30-45 mins. A red pixel represents a vertically developing, newly glaciated cumulus with a cloud-top T_B within the 0 to –20º C range (from the results of RR03). A comparison of the red pixels to future radar imagery at 2030 and 2100

UTC demonstrates the skill of the algorithm, as seen through a comparison of Figs. 2 and 7.

The CI nowcast product identifies future development of the primary convective line in eastern Kansas. Pixels identified in western Missouri also evolved into precipitating convective storms. The nowcast identifies future CI in north-central Kansas, as well as weaker convective growth in southeast Kansas. For this particular case, the nowcast has demonstrated predictive skill in identifying future CI associated with moving convective storms at 30-45 min lead times. Accuracies of approximately 70% are obtained when qualitative pixel-by-pixel comparisons are made between the CI nowcast pixels and radar echoes ≥ 30 dBZ in subsequent imagery. *It must be noted that the premise of the assessment in Fig. 7 is the assumption that linear trends in cumulus development will continue in the future.* Hence, *this algorithm identifies locations where the mesoscale convergent forcing is supporting organized updrafts of sufficient scale to produce precipitation, and the upscale growth of cumulus clouds.*

4. FUTURE WORK

Future efforts will focus on developing a quantitative validation methodology for the CI nowcast product in preparation for this algorithm's introduction into operational use. Also, a statistical analysis of collocated satellite and radar data will be performed to identify the relative contribution of each CI interest field toward an accurate CI nowcast. An examination of the potential contribution of ancillary datasets toward CI nowcasting such as GOES Sounder derived atmospheric stability parameters, NWP model fields, and lightning flash density will also be performed.
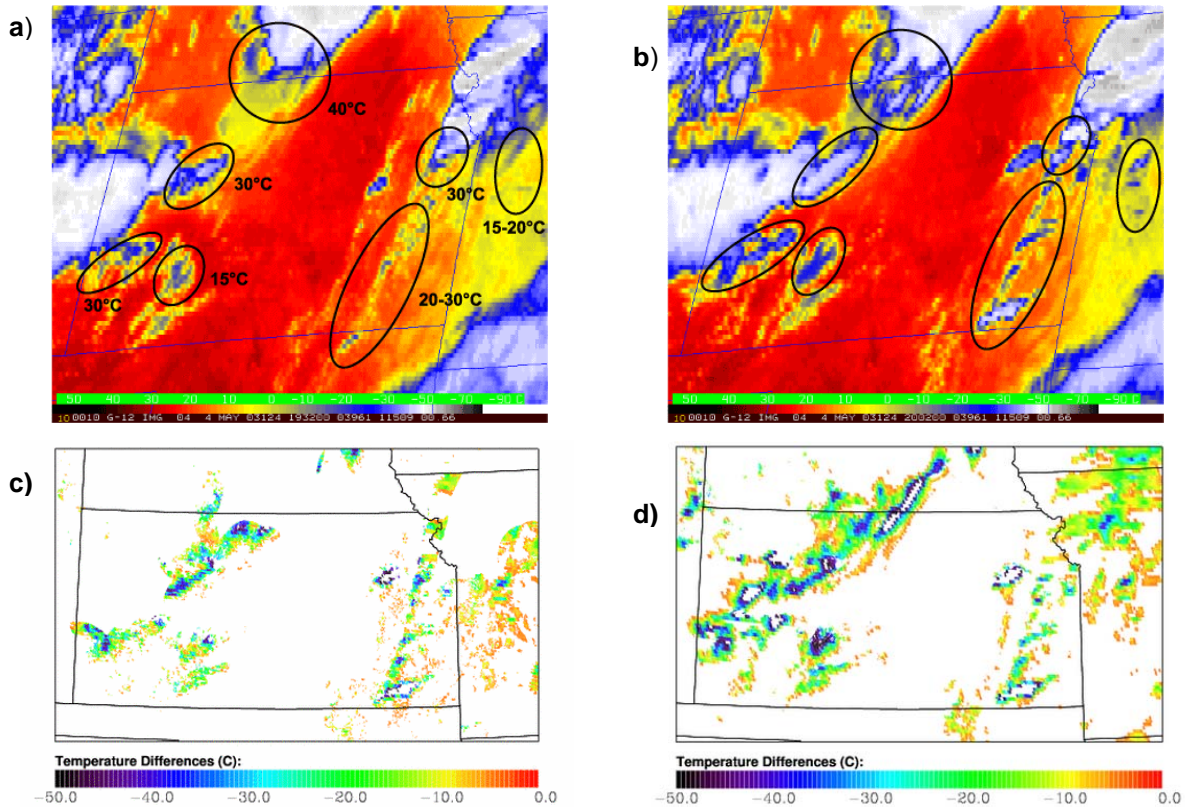
5. ACKNOWLEDGEMENTS

Figure 5: GOES-12 color-enhanced 10.7 mm imagery at: (a) 1930 UTC and (b) 2000 UTC for the 4 May 2003 case. Developing convection is outlined by ovals and the 30 min cooling rates (determined by a human expert) are listed for each distinct growing cumulus cluster in (a). 10.7 μm cooling rates (c) with and (d) without using meso-scale AMVs (i.e. assuming no cloud motion). Shown are time differences less than -4ºC.

CI Interest Field	Critical Value
10.7 μm T_B (1 score)	< 0° C
10.7 μm T_B Time Trend (2 score)	< -4° C/15 mins ΔT_B/30 mins < ΔT_B/15 mins
Timing of 10.7 μm T_B drop below 0° C (1 score)	Within prior 30 mins
6.5 (or 6.7) - 10.7 μm difference (1 score)	-35° C to -10° C
6.5 (or 6.7) - 10.7 μm Time Trend (1 score)	> 3° C/15 mins

Figure 6: A summary of the per-pixel criteria used in the CI nowcast algorithm for GOES-12 satellite data.
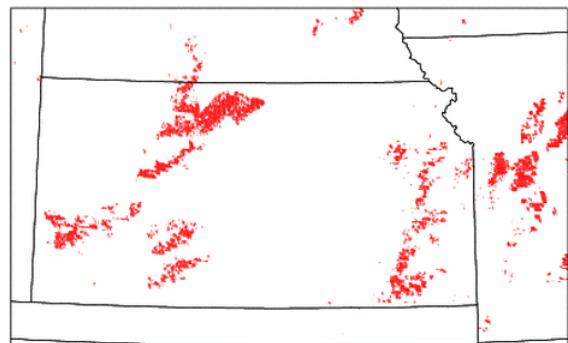

Figure 7: The CI nowcast product valid at 2000 UTC on 4 May 2003. Pixels highlighted in red have met at least five of the six CI criteria (from Fig. 6) and need to be monitored for future CI over the following hour.

6. REFERENCES

Ackerman, S. A., 1996: Global satellite observations of negative brightness temperature differences between 11 and 6.7 μm. *J. Atmos. Sci.*, **53**, 2803-2812.

Barnes, S. L., 1964: A technique for maximizing details in numerical weather map analysis. *J. Appl. Meteor.*, **3**, 396-409.

Bedka, K. M. and J. R. Mecikalski, 2004: Applications of satellite-derived atmospheric motion vectors for estimating mesoscale flows. Submitted to *J. Appl. Meteor.* (August 2004).

Mecikalski, J. R., D. B. Johnson, J. J. Murray, and many others at UW-CIMSS and NCAR, 2002: NASA Advanced Satellite Aviation-weather Products (ASAP) study report, NASA Technical Report, 65 pp. [Available from the Schwerdtferger Library, 1225 West Dayton Street, Univ. of Wisconsin-Madison, Madison, WI 53706.].

------, and K. M. Bedka, 2004: Forecasting convective initiation by monitoring the evolution of moving cumulus in daytime GOES imagery. Accepted for publication in *Mon. Wea. Rev.* (July 2004).

Mueller, C., T. Saxen, R. Roberts, J. Wilson, T. Betancourt, S. Dettling, N. Oien, and J. Yee, 2003: NCAR Auto-Nowcast system. *Wea. Forecasting*: **18**, 545-561.

Murray, J. J., 2002: Aviation weather applications of Earth Science Enterprise data. Earth Observing Magazine, 11, No. 8, (August 2002).

Roberts, R. D., and S. Rutledge, 2003: Nowcasting storm initiation and growth using GOES-8 and WSR-88D data. *Wea. Forecasting*, **18**, 562-584.

Schmetz, J., S. A. Tjemkes, M. Gube, and L. van de Berg, 1997: Monitoring deep convection and convective overshooting with METEOSAT. *Adv. Space. Res.*, **19**, 433-441.

Velden, C. S, C. M. Hayden, S. J. Nieman, W. P. Menzel, S. Wanzong, J. S. Goerss, 1997: Upper-tropospheric winds derived from geostationary satellite water vapor observations. *Bull. Amer. Meteor. Soc.*, **78**, 173-195.

------, T. L. Olander, and S. Wanzong, 1998: The impact of multispectral GOES-8 wind information on Atlantic tropical cyclone track forecasts in 1995. Part I: Dataset methodology, description, and case analysis. *Mon. Wea. Rev.*, **126**, 1202-1218.